Proceedings of the
Annual Stability Conference
Structural Stability Research Council
St. Louis, Missouri, April 16-20, 2013

Calculating the Impact of Partial Warp Restraint on Steel Girder Elastic Buckling Strength

C.E. Quadrato[1], K.A. Arnett[2]

Abstract
The impact of warp-restraint devices on girder elastic buckling strength has typically been estimated by assuming no warp restraint or total warp restraint at both ends of the girders. However, neither of these conditions is typically present in steel bridge construction. In a typical steel bridge, even one with warp restraining devices, two ends of any given girder segment will be restrained to different degrees by a warp restraining device at the abutment or pier and by any adjacent segments in the span of the bridge.

Previous research has shown the large impact warp restraint has on girder elastic buckling strength. In particular, large scale buckling tests at the University of Texas at Austin Ferguson Structural Engineering Laboratory with subsequent computational studies, and an energy solution proposed by Trahair have resulted in methods to analytically estimate the increase in buckling strength. However, these methods have not been applied to continuous girders where the end restraints on the critical span may differ and include warp restraining devices. This paper investigates these conditions using a series of parametric studies with a previously validated finite element model and proposes a method to account for the increase in elastic buckling strength due to a split pipe warp restraining devices at the abutments and intermediate piers of continuous span girders.

1. Introduction

Previous research regarding warp restraining devices has focused on the warp restraint provided to single span girders with simple supports but has overlooked the device's impact on a continuous span girder. This paper uses a previously validated finite element model to perform parametric studies to explore these two specific continuous girder geometries and proposes a possible analytic procedure to calculate such increases.

While using warp restraint devices on individual simple spans has been shown to significantly increase elastic stability (Quadrato, Frank, Helwig, & Engelhardt, 2010), such devices have a very good probability of having a similar effect when used at the piers of continuous spans.

[1] Assistant Professor, United States Military Academy, <craig.quadrato@usma.edu>
[2] Instructor, United States Military Academy, <kevin.arnett@usma.edu>

2. Background

Using continuous girders not only provides benefit in distributing moments and deflections with respect to the girder's strong axis, they also allow one segment to provide warping restraint and weak axis rotational restraint to a more critical adjacent segment and thereby increase the elastic buckling capacity of the critical segment. This interaction between adjacent spans is shown in the picture below (the girder shown is the three-span model using the D48 cross section described in a later section).

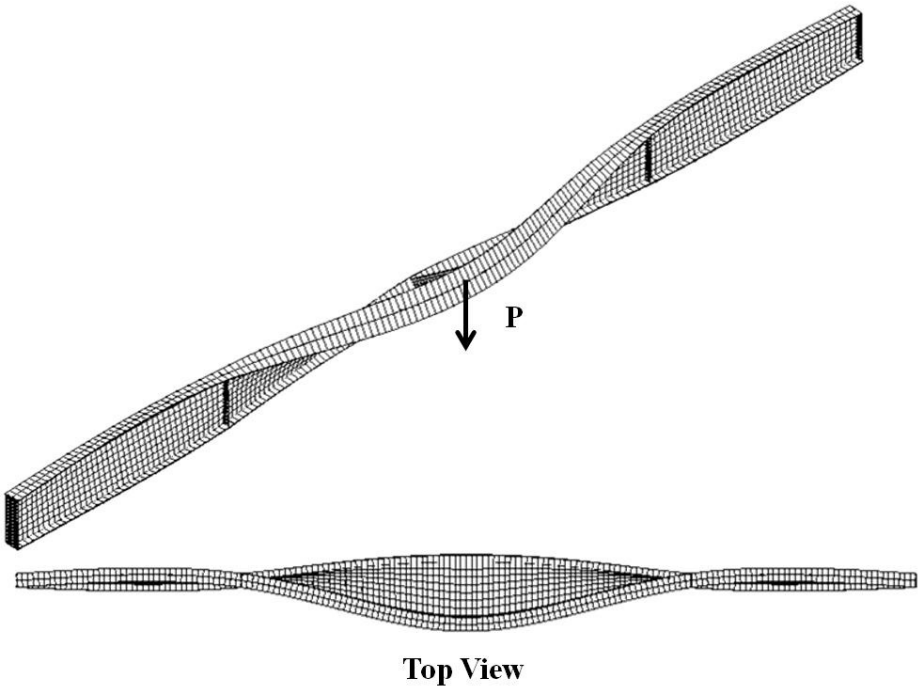

Figure 1: Three-Span Girder Buckled Shape with Plate Bearing Stiffeners

The adjacent segments brace the critical segment in two ways. First they restrict the weak axis rotation of the critical segment ends. By doing so, they increase critical segment buckling strength by stiffening the critical segment against translation. If the governing buckling mode is lateral-torsional buckling (this mode pairs a twisting and translation of the critical girder segment as shown above) then the critical segment buckling load will increase. Second, the adjacent restraining spans also provide warping restraint. In order for the cross section to twist about the longitudinal axis of the girder (as shown in the center span of the top view in Fig. 1), the top and bottom flange must bend in their strong planes opposite one another. However, due to the presence of the adjacent spans, the critical span flanges cannot warp freely at their ends. Instead the warping stiffness of the adjacent spans restrains them. This is why in the unloaded end spans in the picture above, the flanges are bending opposite of those in the critical span. This further increases the critical span's elastic buckling strength.

A split pipe, welded to each side of the girder web, at the abutments and piers, also provides warping restraint to the critical and restraining spans. It does so by bracing the top flange rotation against the bottom flange. In order for the flanges to warp, they must twist the pipe.

Since the pipe is torsionally stiff, a pipe can be a significant source of stability and dramatically increase the elastic buckling capacity of the critical segment. An example is shown in Fig.2 below. By comparing the split pipe top view with that of the plate stiffener model it can be seen that the flanges of the restraining spans do not warp nearly as much in the split pipe stiffened model. This is because the pipe is providing significant warping restraint and keeping the flanges from bending in opposite directions.

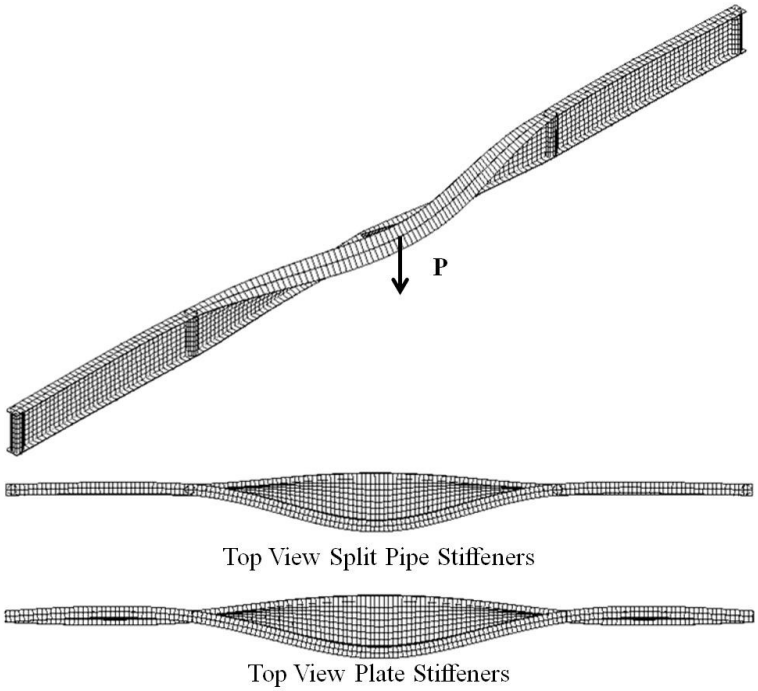

Figure 2: Three-Span Girder Buckled Shape with Split-Pipe Bearing Stiffeners (plate stiffened top view shown at bottom for comparison)

While there has been significant research in accounting for the warp restraint provided to the critical segment from adjacent segments, as summarized in Chapter 5 of the *Guide to Stability Design Criteria for Metal Structures* (SSRC, 1998), no analytical method has been investigated to incorporate warp restraining devices with continuous girders. To do so requires determining how to account for the warp restraint provided by adjacent restraining spans and the warp restraining device, and how to account for differing warp restraint conditions on the ends of the critical and supporting segments. This paper describes the initial attempt to do so for a split pipe stiffener and shows how effective a split-pipe stiffener is in increasing the elastic buckling strength of the girder's critical span.

3. Finite Element Models and Parametric Study

Two finite element models were used in this study. The first was a two span system and the second a three span system. All were modeled in the three-dimensional finite element modeling program ANSYS using 8-node shell elements (SHELL93). Such techniques have been previously validated using laboratory tests and well-known analytic solutions (Quadrato, Frank, Helwig, & Engelhardt, 2010), (Quadrato, et al., 2010). Each of the three models was analyzed

using an eigenvalue buckling analysis with the five doubly symmetric cross sections pictured below for critical span-to-depth ratios of 20 to 40.

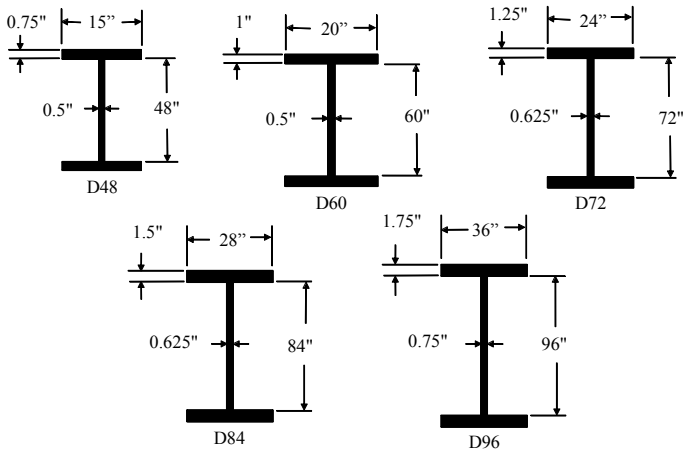

Figure 3: Cross Sections Used in Parametric Study

All models were simply supported at the abutments and piers. No twist was allowed at the abutments and piers. Pipe diameters used were two inches less than the flange width for the D48 and D60 cross sections and four inches less than the flange width for all other cross sections. Pipe and plate bearing stiffeners were ½” thick, and plate stiffeners were used at the point of application of all concentrated loads. The two models are explained in more detail below.

3.1 Two-Span Model

This model had two symmetric spans. One span had a point load at mid-span and the other was unloaded. The loaded span was the critical span due to its moment diagram and was braced by the unloaded span. The point load was positioned on the top flange and the model was run with plate and split pipe stiffeners. A picture of the two-span model with loading and support condition annotations is shown below.

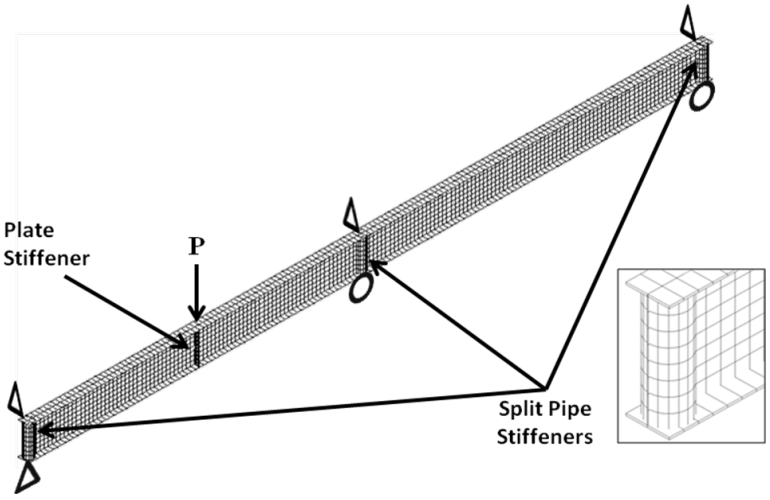

Figure 4: Two Span Girder Model with Split-Pipe Bearing Stiffeners (inset)

3.2 Three-Span Model

The three-span model had a center span and two end spans that were half the length of the center span. The loading condition used was a concentrated load at the midpoint of the center span. This caused the middle span to be critical and it was braced symmetrically by the end spans. A picture of the three-span model with loading and support conditions is shown below.

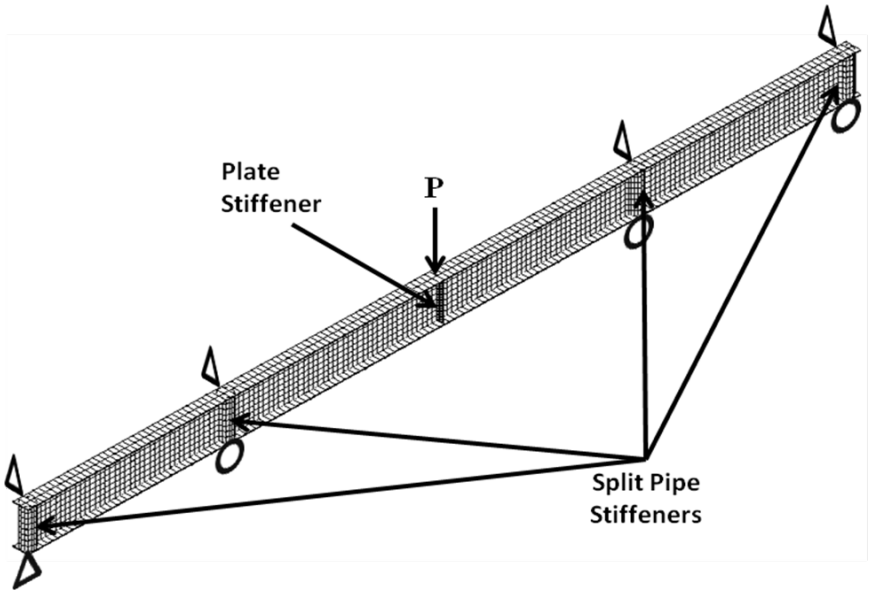

Figure 5: Three Span Girder Model with Split-Pipe Bearing Stiffeners

4. Proposed Analytic Solution for Continuous Girders Using Split Pipe Stiffeners

The proposed analytic solution for calculating the elastic buckling strength for continuous girders using split pipe stiffeners is adapted from the procedure found in Chapter 10 of *Flexural-Torsional Buckling of Structures* (Trahair, 1993) and is given below. The expression for the pipe warping restraint stiffness (α_{wpipe}) is adapted from (Pi & Trahair, 2000). The procedure below accounts for the interaction of the critical span and the restraining spans adjacent to it. Since the critical and adjacent spans have to buckle in a girder simulaneously, estimating buckling capacity using the procedure below will more closely approximate a girder's actual buckling strength rather than assuming no interaction between adjacent spans during buckling.

1. Compute the girder strong axis bending moment diagram and find the maximum moment in each segment (M_{mi}) for the load condition to be investigated.

2. Calculate the effect of moment gradient and load height using the method outlined in The Guide to Stability Design Criteria for Metal Structures (SSRC, 1998) for each segment assuming the segment is simply supported as shown in sub-steps a and b below.

    a. For spans with loads transverse to the girder longitudinal axis

$$C_{bi} = AB^{2y/h} \tag{1}$$

where

A = 1.35 for simply supported girder with point load at mid-span
B = 1-0.018W^2+0.649W
W = $\pi/L_b\sqrt{((EC_w)/(GJ))}$, where L_b, E, C_w, G, and J defined below
y = distance from load point to cross section mid-height (positive for below and negative for above cross section mid-height)
h= girder depth

b. For spans with no loads transverse to the girder longitudinal axis

$$C_{bi} = \frac{12.5M_{\max}}{2.5M_{\max} + 3M_A + 4M_B + 3M_C} \tag{2}$$

where

M_{max} = maximum moment in the span
M_A, M_B, M_c = the moments at the ¼, ½, and ¾ points in the span, respectively

3. Determine the critical elastic buckling moment capacity (M_{cri}) for each unbraced segment using Eq. 3 (American Institute of Steel Construction, 2001) and (Trahair, 1993) assuming no warping or weak axis rotational restraint is provided by adjacent spans or the split pipe stiffener (k_y and k_w equal to one). This is known as the no-interaction condition since it assumes each span buckles independent of the others.

$$M_{cri} = C_{bi} / (k_y L_b)\sqrt{EI_y GJ + \pi^2 E^2 C_w I_y / (k_w L_b)^2} \tag{3}$$

where

M_{cri} = girder segment buckling moment
C_{bi} = girder segment moment gradient coefficient
L_b = girder segment unbraced length
I_y = girder segment weak-axis moment of inertia
G = shear modulus
J = girder segment torsional constant
E = Young's modulus
C_w = girder segment warping constant
k_y = girder segment effective length factor for weak axis rotational restraint
k_w = girder segment effective length factor for warping restraint

4. Determine each segment's remaining load capacity prior to elastic buckling for the loading condition to be investigated using Eq. 4 below. The highest value of λ will be the critical segment (λ_c) and the segments adjacent to it will be the restraining segments $(\lambda_r)_{A/B}$ where A and B denote the segments on either side of the critical segment.

$$\lambda_i = M_{cri} / M_{mi} \tag{4}$$

where

λ_i = segment buckling capacity factor

5. Determine the bending moment distribution factor (γ_r) for restraining segments A and B using Eq. 5 below.

$$\gamma_f = (1 - M_{mr}{}^2 / M_{crr}{}^2)_{A/B} \tag{5}$$

where

M_{mr} = bending moment in restraining segment A or B from step 1.
M_{cr} = elastic moment capacity in restraining segment A or B from step 2

6. Compute restraint stiffness for the critical segment, supporting segments, and split pipe stiffeners as shown in sub-steps a – d below.

    a. Critical segment weak axis flexural stiffness (α_c)

$$\alpha_{cy} = (n/2)EI_y / L_b \tag{6}$$

    where

    n = 4 if both ends are continuous or 3 if only one end is continuous

    b. Critical segment warping stiffness

$$\alpha_{cw} = EC_w / L_b \tag{7}$$

    c. Restraining segments A and B restraint stiffness

$$\alpha_{rA/B} = \gamma_f EI_y / L_b(1 - \lambda_c / \lambda_r) \tag{8}$$

    d. Split pipe warping restraint stiffness

$$\alpha_{pipe} = GJ_{pipe}d \tag{9}$$

    where

    d = distance between bottom and top flange centroids

7. Determine the stiffness ratios ($G_{A/B}$) for weak axis rotational restraint and warping at the A and B ends of the critical segment as shown in sub-steps a and b below.

    a. Restraining segments A and B and pipe warping restraint stiffness ratio. If pipe warping restraint stiffness (α_{pipe}) is small compared to that of the restraining span

warping stiffness (EC_w/L_b), the value for the restraining span warping restraint stiffness should be added to that of the pipe in the denominator in the equation below.

$$G_{wA/B} = \alpha_{cw} / (\alpha_{pipe}) \tag{10}$$

b. Restraining segments A and B weak axis rotational restraint stiffness ratio

$$G_{yA/B} = \alpha_{cy} / \alpha_{rA/B} \tag{11}$$

8. Solve for the effective length factors for weak axis rotation restraint (k_y) and warping (k_w) by using the appropriate restraint stiffness ratios and iterating to solve the equation below for k.

$$\frac{G_A G_B}{4}\left(\frac{\pi}{k}\right)^2 + \left(\frac{G_A + G_B}{2}\right)\left(1 - \frac{\frac{\pi}{k}}{\tan\left(\frac{\pi}{k}\right)}\right) + \frac{2\tan\left(\frac{\pi}{2k}\right)}{\frac{\pi}{k}} = 1 \tag{12}$$

9. Determine the critical segment elastic bucking moment capacity considering adjacent span and split pipe stiffener warp restraining device (M_{cr}) using the effective length factors from step 8 in Eq. 3.

5. Analytical and Finite Element Model Results.

All models and analytic solutions were run using the cross sections shown in Fig. 3, and the results of the analytical solutions and finite element model solutions were normalized against the no interaction critical load for the critical span of the girders previously described. The results for each model and its analytic solution are given below.

5.1 Two-Span Model

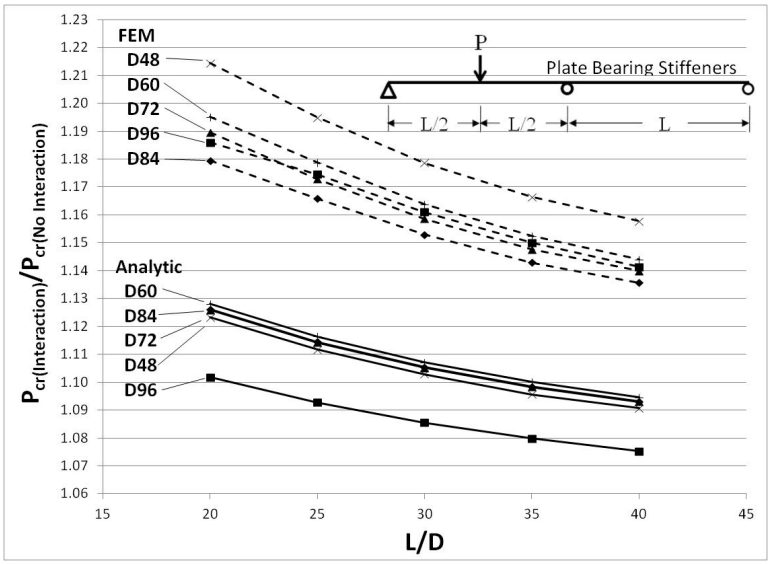

Figure 6: Two Span Girder Model with Plate Bearing Stiffener Results

From Fig. 6 it can be seen that the analytic solution is within 10% of the finite element model solution. Most of this error can be attributed to the estimate of C_b. Eq. 1 assumes a no interaction case and will therefore underestimate the actual buckling load. However since the error is relatively small and conservative, the existing procedure gives a good estimate for the loading and specimen geometry in the two span case. Additionally it can be seen that accounting for the stiffening provided by the unloaded span gives an increase from 15% to 20% in elastic buckling capacity from the no-interaction case.

If a split pipe stiffener is used at the bearings and piers, the increase in elastic buckling strength is much larger. The results of the split pipe stiffened models and analytic solutions are shown in Fig. 7 below.

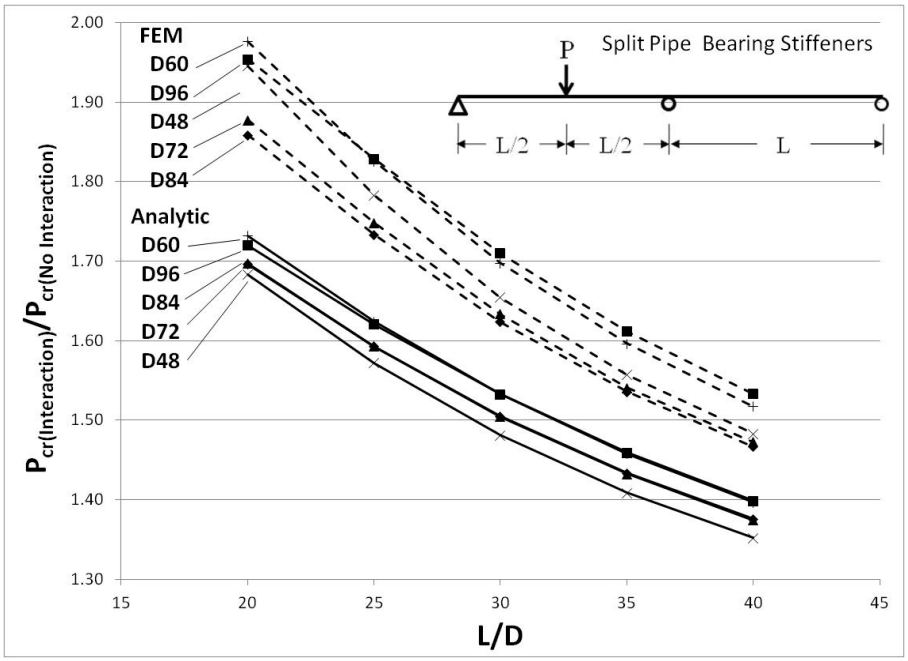

Figure 7: Two Span Girder Model with Split Pipe Bearing Stiffener Results

From Fig. 7 it can be seen that the pipe stiffener increases the elastic buckling capacity an additional 30% to 70% over the support provided by the unloaded span alone. This is due to the large torsional restraint the pipe provides to both spans.

We also see that the analytic solution is again about 10% and sometimes nearly 15% conservative when compared to the finite element model. Most of this error is due to the underestimate of C_b previously mentioned in the two-span model discussion; however, there is also an error in the pipe warping restraint estimate as well.

By using the ratio of the warping stiffness of the critical segment (EC_w/L_b) to torsional stiffness parameter of the pipe (GJd) in Eq. 12, we are assuming that the warping restraint of the pipe is applied at the end of a simple span where the flange warping is at a maximum. But, since the adjacent span stiffens the loaded span, the point of maximum warping moves away from the pier into the critical span. This decreases the effective restraint of the pipe against warping.

The error is conservative and relatively small, therefore it is tolerable; however, in other geometries this may not be the case. One such geometry is a three span system where the adjacent spans are much stiffer than the critical span. This is the case with the three span model discussed in the next section.

5.2 Three-Span Model

If the analytic procedure described above is used, the resulting elastic buckling strength with and without the pipe stiffener is in error, and that error is not consistent. As shown in the figure below for the D60 cross section, the current analytic procedure inconsistently over and under predicts the elastic buckling strength with and without the pipe stiffener. This pattern is consistent among all cross sections investigated. The most likely causes are the inaccuracies in the C_b calculation and the position of the split pipe bearing stiffeners at the piers relative to the location of maximum flange warping. To get a better estimate, both these sources of error will be adjusted as described below.

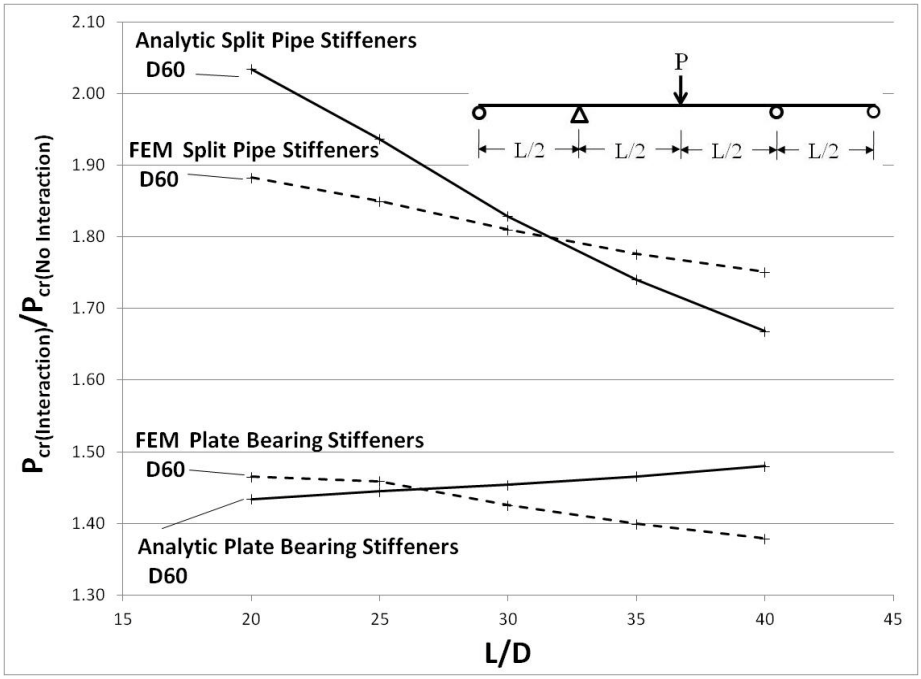

Figure 8: Three Span Girder Model Results

To adjust C_b, we will simply adjust the portion of the moment diagram under consideration. In order to do this, we will use the effective length for weak axis rotation (k_yL_b) initially calculated in step 8 for the C_b calculation in the critical span using Eq. 1 and then repeat the analytic procedure with this updated C_b estimate. The results for three of the cross sections in the plate stiffened sections given below show good agreement between the finite element and analytic procedure using the improved C_b estimate. The other two cross sections showed similar good agreement. Of course, further iteration could be performed, but in this study further iteration did not significantly improved the results shown below.

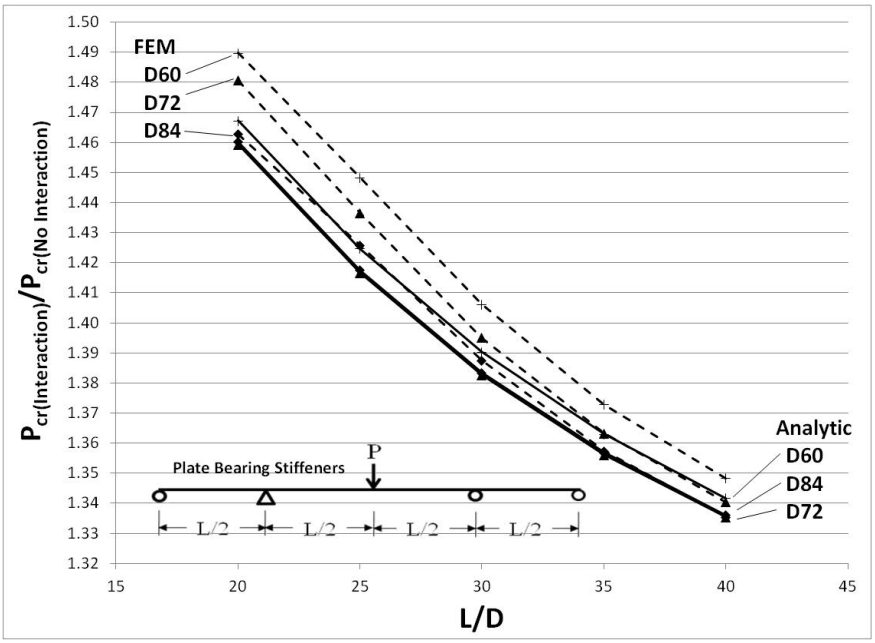

Figure 9: Three Span Girder Plate Bearing Stiffener Model Adjusted Results

From the results above it can be seen that the improved C_b estimate results in no more than a consistent 3% error in the elastic buckling strength when considering interaction between the spans. Additionally it can be seen that the buckling strength of the critical span is increased by 33% to nearly 50% by accounting for the buckling interaction between spans.

To account for the positioning of the pipe away from the point of maximum warping, an estimate of variation of flange warping along the length of the critical span must be made. By conservatively assuming simple torsional support at the ends of the critical span, the variation of flange warping varies along the length of the span as shown below (Salmon & Johnson, 1996).

$$\beta = \frac{\cosh(\omega z)}{\cosh(\omega L_b / 2)} \tag{13}$$

where

β = warping restraint reduction factor
$\omega = (GJ/(EC_w))^{1/2}$
z = distance from the start of critical span to flange lateral bending inflection point (we estimate this by using the effective length for warping such that $z = L_b(1-k_w)/2$ in this symmetric example – an initial estimate of k_w may be made by assuming $\beta = 1$).

The following modifications may now be made to the procedure previously described. After getting an initial estimate for the warping effective length factor (k_w) including the pipe in the original procedure above, Eq (7) is modified as shown below. This modification accounts for the reduction in the effective warping length of the critical segment.

$$\alpha_{cw} = EC_w / (k_w L_b) \tag{7a}$$

Next Eq. (10) is modified in two ways. First, to account for the pipe not being at the point of maximum warping due to the interaction of the adjacent spans, the pipe warping restraint stiffness (α_w) is multiplied by the warping restraint reduction factor (β). Then to account for the warping restraint of the two adjacent spans (A and B) the denominator is increased by their warping stiffness.

$$G_{wA/B} = \alpha_{cw} / (\beta \alpha_{pipe} + (EC_w / (L_b))_{A/B}) \tag{10a}$$

The above procedure requires two or three iterations until an accurate estimate is found. The results of using this modified procedure are shown below for the D48 and D84 cross sections. . As can be seen from the figure, the improved analytical procedure results an estimate in increase in elastic buckling load that differs from the finite element model by only 1% to 5%. These results are similar for all cross sections in the study. Additionally, the figure shows the increase in elastic buckling capacity when using the split pipe stiffener at intermediate piers is dramatic. Similar gains in elastic buckling strength from 55% to 90% at span-to-depth ratios of 20 to 40, respectively, were found in all cross sections studied.

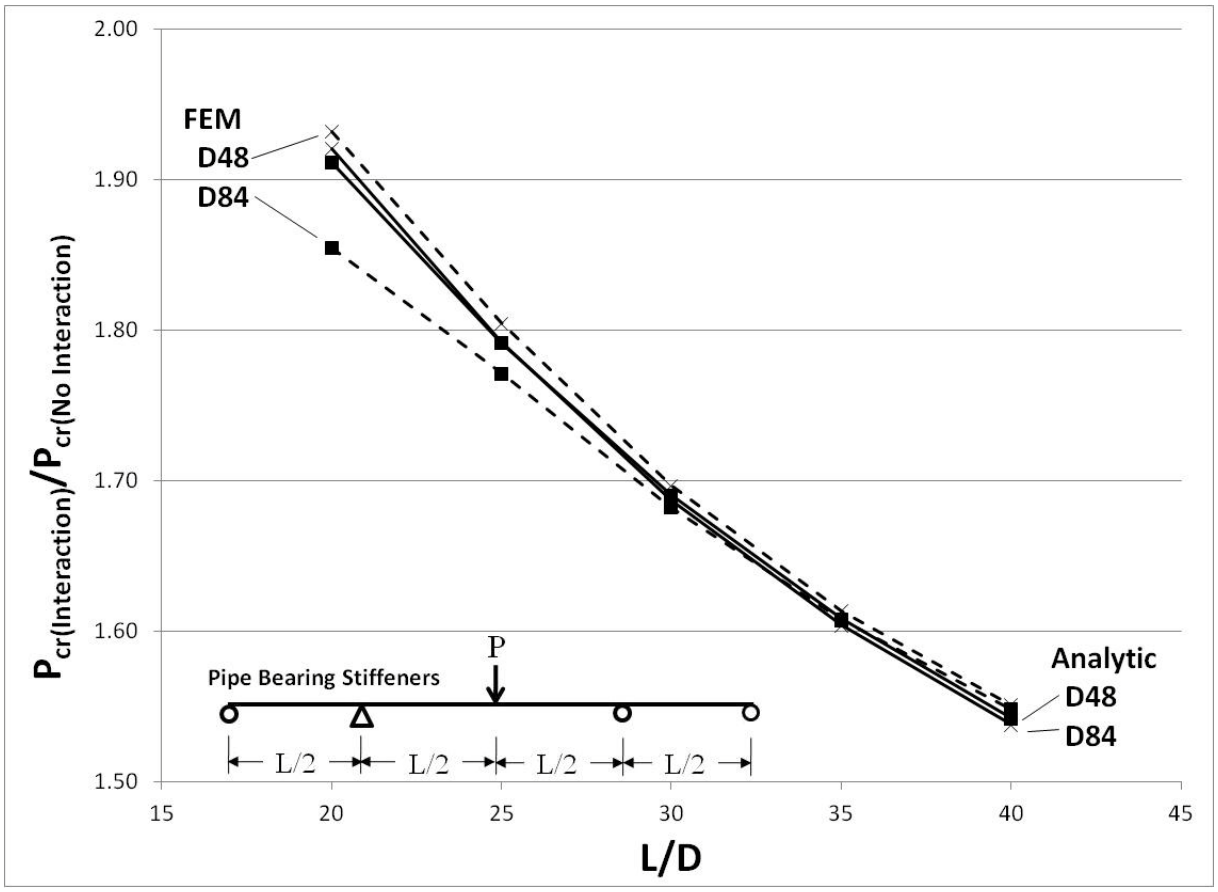

Figure 10: Three Span Girder Pipe Bearing Stiffener Model Adjusted Results

6. Conclusions.

This study has shown that the split-pipe bearing stiffener is very effective in increasing the elastic buckling capacity of the critical span in a continuous girder. Such increases were about 50% in span-to-depth ratios of up to 40 and as high as 90% in span-to-depth ratios of 20. This study proposed a general analytic procedure to estimate these increases that accounts for the interaction of the adjacent spans and split-pipe bearing stiffener in terms of warping and weak axis lateral rotation restraint. While further study is required to investigate other loading conditions and other typical girder geometries, this initial study shows great promise for the use of split-pipe bearing stiffeners on continuous girders.

References

American Institute of Steel Construction. (2001). *Manual of Steel Construction.* Chicago: American Institute of Steel Constrution.

American Institute of Steel Construction. (2011). *Manual of Steel Construction.* Chicago: American Institute of Steel Constrution.

Pi, Y.-L., & Trahair, N. S. (2000). Distortion and Warping at Beam Supports. *Journal of Structural Engineering* , 1279-1287.

Quadrato, C. B., Frank, K., Helwig, T., & Engelhardt, M. (2010). Improved Cross-Frame Connection Details for Steel Bridges with Skewed Supports. *Transportation Research Record Journal of the Transportaion Research Board* , 29-35.

Quadrato, C., Wang, W., Battistini, A., Wahr, A., Helwig, T., Frank, K., et al. (2010). *Technical Report 0-5701-1 Cross-Frame Connection Details for Skewed Steel Bridges.* Austin: Center For Transportation Research.

Salmon, C. G., & Johnson, J. E. (1996). *Steel Structures Design and Behavior.* Upper Saddle River: Prentice-Hall Inc.

Structural Stability Research Council. (1998). *Guide to Stability Design Critiera for Metal Structures*. (T. V. Galambos, Ed.) New York: Wiley & Sons.

Trahair, N. S. (1993). *Flexural-Torsional Buckling of Structures.* Boca Raton: CRC Press.